

## Architecture of the upgraded BCM1F backend electronics for Beam Conditions and Luminosity measurement

This content has been downloaded from IOPscience. Please scroll down to see the full text.

2015 JINST 10 C02020

(<http://iopscience.iop.org/1748-0221/10/02/C02020>)

View [the table of contents for this issue](#), or go to the [journal homepage](#) for more

Download details:

IP Address: 131.169.4.70

This content was downloaded on 08/01/2016 at 08:27

Please note that [terms and conditions apply](#).

TOPICAL WORKSHOP ON ELECTRONICS FOR PARTICLE PHYSICS 2014,  
22–26 SEPTEMBER 2014,  
AIX EN PROVENCE, FRANCE

## Architecture of the upgraded BCM1F backend electronics for Beam Conditions and Luminosity measurement

A.A. Zagodzinska,<sup>a,b,1</sup> A.E. Dabrowski,<sup>a</sup> D. Przyborowski,<sup>c</sup> J.L. Leonard,<sup>d</sup>  
K.T. Pozniak,<sup>b</sup> M. Miraglia,<sup>a,e</sup> R. Walsh,<sup>d</sup> W. Lange,<sup>d</sup> W. Lohmann<sup>d,f</sup> and V. Ryjov<sup>a</sup>

<sup>a</sup>CERN, Geneva, Switzerland

<sup>b</sup>Warsaw University of Technology, Warsaw, Poland

<sup>c</sup>AGH University of Science and Technology, Warsaw, Poland

<sup>d</sup>DESY, Zeuthen, Germany

<sup>e</sup>Università di Pisa and INFN – Sezione di Pisa, I-56100 Pisa, Italy

<sup>f</sup>Branderburg University of Technology, Branderburg, Germany

E-mail: [a.zago@cern.ch](mailto:a.zago@cern.ch)

**ABSTRACT:** The Beam Radiation Instrumentation and Luminosity Project of the CMS experiment consists of several beam monitoring systems and luminometers. The upgraded Fast Beam Conditions Monitor is based on 24 single crystal diamond sensors with a two-pad metallization and a custom designed readout. Signals for real time monitoring are transmitted to the counting room, where they are received and processed by new back-end electronics designed to measure count rates on LHC collision, beam induced background and activation products to be used to determine the luminosity and the machine induced background. The system architecture and the signal processing algorithms will be presented.

**KEYWORDS:** Detector control systems (detector and experiment monitoring and slow-control systems, architecture, hardware, algorithms, databases); Modular electronics; Beam-line instrumentation (beam position and profile monitors; beam-intensity monitors; bunch length monitors); Diamond Detectors

<sup>1</sup>Corresponding author.

---

## Contents

|          |  |          |
|----------|--|----------|
| <b>1</b> | <b>Overview of the CMS Fast Beam Condition Monitoring system</b> | <b>1</b> |
| 1.1      | Back-end electronics architecture                                | 3        |
| 1.2      | Frontend detector configuration and control                      | 4        |
| <b>2</b> | <b>Data rates</b>  | <b>4</b> |
| 2.1      | Raw data   | 5        |
| 2.2      | Time domain histogram  | 5        |
| 2.3      | The amplitude monitor of the gain                                | 5        |
| 2.4      | Total data production in Lumi Nibble                             | 6        |
| <b>3</b> | <b>Identification of the hits</b>                                | <b>6</b> |
| 3.1      | Time and amplitude measurement methods                           | 7        |
| 3.2      | Baseline monitoring  | 8        |

---

## 1 Overview of the CMS Fast Beam Condition Monitoring system

The increased performance of the LHC with a collision energy of up to 14 TeV, higher luminosity and 25 ns bunch spacing will increase the importance of real-time monitoring at high rates. The upgraded Fast Beam Condition Monitoring (BCM1F) system is a part of the CMS Beam Radiation Instrumentation and Luminosity Project (BRIL). It is designed to monitor the flux and timing of the particles originating from the proton-proton interactions and machine induced background (MIB) particles. The frontend modules consist of 24 single crystalline CVD diamond sensors on two parallel planes positioned at the distance of  $z = \pm 1.83$  m away from the interaction point (IP), mounted radially at  $r = 7.2$  cm from the beam line. Each  $5 \text{ mm} \times 5 \text{ mm} \times 500 \mu\text{m}$  diamond has a two pad metallisation with  $25 \mu\text{m}$  split that will decrease the hit probability of a single channel. The distance between the sensors and the IP is optimal for the separation of incoming and outgoing particles and corresponds to the time-of-flight of 6.25 ns for relativistic particles as is shown in figure 1. The hits originating from collisions, MIBs and activation will be classified using its arrival time. The corresponding count rates will be used to measure in real time the luminosity, background and activation product rates [1].

Figure 2 shows the data transmission path. The diamonds are mounted to the dedicated front-end ASIC comprising of a fast transimpedance preamplifier with active feedback, shaper stage, and high-performance output buffer [2]. For a sensor capacitance of 2 pF, the ASIC produces pulses with a peaking time of 7 ns and full width at half maximum (FWHM) of 9 ns. The minimal two hit time resolution is 12.5 ns. The diamonds and the front-end electronics are mounted on complex flex-rigid PCBs. These PCBs will be held by a carbon-fibre carriage and mounted in the pixel service tube. Each of four PCBs has four Analogue Opto-Hybrids (AOH) [3] for optical conversion, and one Digital Opto-Hybrid (DOH) for configuration and control. Signals from the front-end will

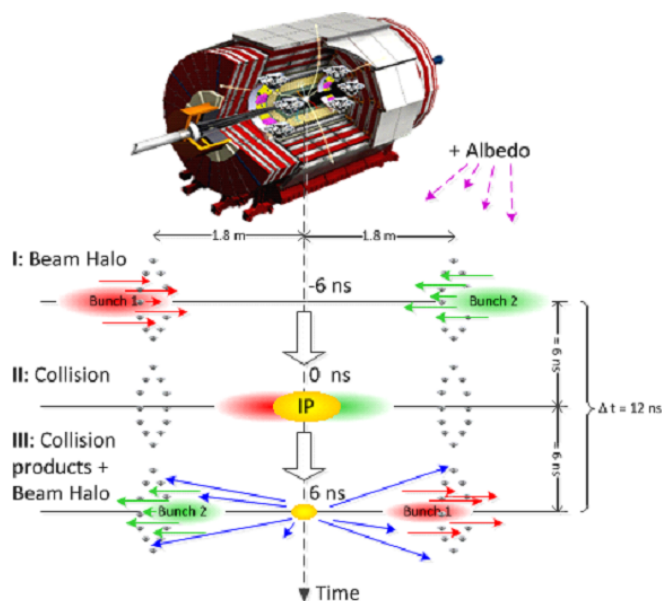


**Figure 1.** The position of the BCM1F detector with respect to the IP, allows for a good separation of collision products from incoming machine induced background (MIB/Beam Halo) and activation products (Albedo), by exploiting the time arrival difference of particles.

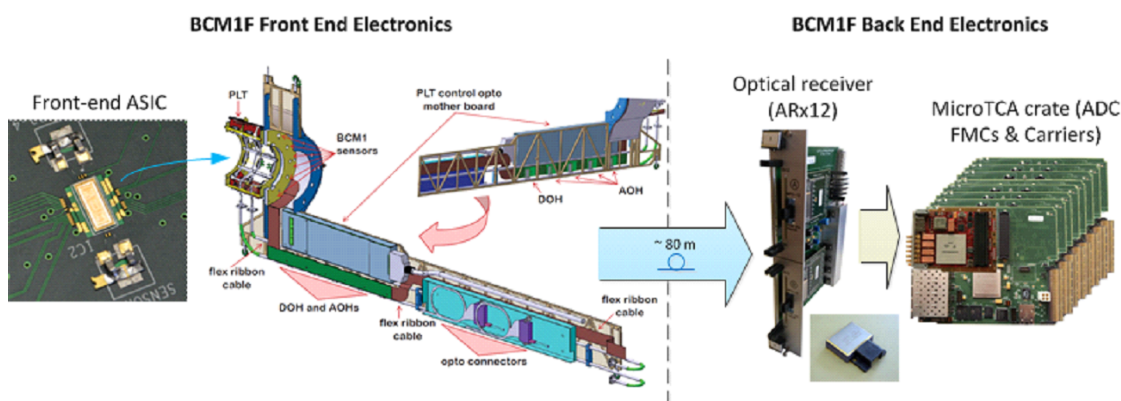


**Figure 2.** Signals from the diamond detectors with the front-end ASICs are mounted on the complex flex-rigid PCBs held by a carbon-fiber carriage. Signals will be transmitted to the counting room where they will be processed by the back-end electronics.

be sent through approximately 80 m of single mode optical fibers to the counting room where they are received by four 12-channel Analogue Receiver Modules (ARx12). Analogue to digital conversion will be performed by twelve 4-channel FMC mezzanines with 8-bit ADCs at a 1.25 GS/s sampling rate (FMC125, 4DSP), mounted on the AMC Gigabit Link Interface Board (GLIB) [4] carriers with HPC FMC connectors. Two additional mezzanines configured for a single channel operation at a 5 GS/s sampling rate will be used for a measurement of the signals from the Beam Pick-up Timing for Experiments (BPTX) [5] detectors. The data processing will be performed in the MicroTCA based back-end electronics that is described in details in the next section.

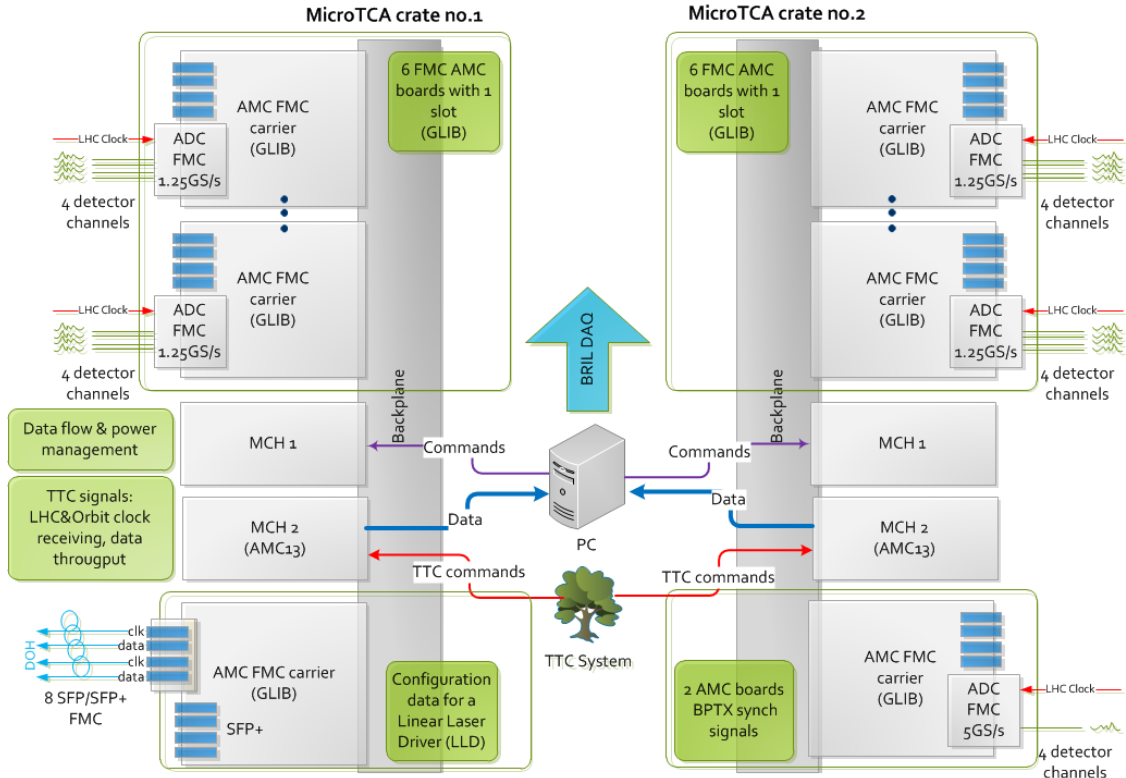


**Figure 3.** Architecture of the upgraded BCM1F backend electronics is based on the MicroTCA technology. The system control and communication will be operated by the specialized CMS MicroTCA Hub module AMC13.

### 1.1 Back-end electronics architecture

Architecture of the upgraded BCM1F backend electronics is based on the MicroTCA technology [6]. The system control and communication will be operated by the specialized CMS MicroTCA Hub module AMC13 (AMC13 XG). The module uses a 10 Gbit/s Ethernet based IPbus communication [7] for transferring the large amount of the data. The data flow and the system architecture are presented in figure 3.

The system will use 2 MicroTCA crates. Each of them will contain 6 GLIB AMC carriers with High-pin count (HPC) FMC connectors mounted. This allows the use of 4 ADC channels of the FMC125 mezzanines at the maximum rate. To synchronize these modules the LHC clock will be provided to the mezzanines through the front panel. The 8-bit samples will be transmitted through FMC connectors to the FPGAs mounted on the AMC carriers. The details of the processing modules are described in section 3. The timing information and control commands will be received from the Trigger, Control and Distribution System (TCDS) [8] for CMS. The signals will be decoded by the AMC13 modules and transmitted through the backplanes to all GLIB modules. The processing FPGA will use this information for synchronization and classifying the incoming data. Two types of histograms will be collected during a CMS Lumi Nibble (LN).<sup>1</sup> A minimum of

<sup>1</sup>LN — Lumi Nibble, 2<sup>12</sup> LHC Orbits, 368.23 ms.

one orbit of a raw data each Lumi Nibble will be stored to provide an input for the offline statistic processing. During the data collecting, without introducing any dead time, data from a previous LN will be transmitted to the AMC13 through the backplane and subsequently to the BRIL DAQ. The details concerning the data storage and transmission rates are described in section 2.

A separate branch of the processing applies to signals from the BPTX detector. The BPTX detector uses two standard LHC beam position monitors (BPM) each comprising of four electrostatic button electrodes positioned symmetrically around the beam-pipe. Comparison of timings from opposite beam position monitors gives the highly accurate measurements of the longitudinal interaction point and bunch timing relative to the CMS clock. For this purpose 2 GLIB boards with FMC125 modules will be installed in one of the crates. The mezzanines will be configured in a 1-channel working mode with the maximum 5 Gs/s of the sampling rate.

The last important element of the system will be the readout monitoring. For this purpose the GLIB board with a custom FMC mezzanine EDA-02707-V1 that hosts eight sockets for SFP optical modules operating at up to 800 Mbit/s each will be installed. The details of the implementation are described in the following section.

## 1.2 Frontend detector configuration and control

The module provides signals for control and configuration of the Linear Laser Drivers (LLD) [9] of the AOHs and DOH being the part of the front-end. The module as well as the frontend electronics will be common for two readout systems: a VME based BCM1F that is being developed on the basis of the previous system [10, 11] and the experimental MicroTCA based readout that is the subject of this paper. The monitoring system is based on the CMS CACTUS environment which provides an IPbus communication between the software and FPGA. The application allows for configuration of the bias current and gain setting of the lasers. The lasers will operate in a high radiation field, so the parameters will change with accumulated radiation dose and corrections will be needed. The firmware driver communicates with the AOHs/DOH through the optical links. For this reason the FMC mezzanine EDA-02707-V1 housing 8 optical COTS (Commercial of the Shelves) SFP transceivers is mounted on the GLIB AMC. The optical signals are converted to electrical signals by the DOH and then sent to the Slow Hub ASIC [12]. The chip converts the coded data to the I2C commands for LLD, activates one of the 7 possible output channels and sends the configuration. The hub has been designed for the Forward Pixel Detector.

## 2 Data rates

The LHC upgrade has the several implications to the BCM1F system. During Run I the characteristic instantaneous luminosity of  $5 \times 10^{33} \text{ cm}^{-2}\text{s}^{-1}$  correspond to a hit rate of  $3.7 \times 16 \text{ s}^{-1}$  per sensor ( $1.5 \times 10^7 \text{ cm}^{-2}\text{s}^{-1}$ ) and a sensor occupancy of 12% as measured. For Run II the instantaneous luminosity is foreseen to increase to around  $2 \times 10^{34} \text{ cm}^{-2}\text{s}^{-1}$ , corresponding to a hit rate of  $7.5 \times 10^6 \text{ s}^{-1}$  per sensor ( $3 \times 10^7 \text{ cm}^{-2}\text{s}^{-1}$ ) and sensor occupancy of about 25%. The expected input hit rate of about 300 MHz (for a beam pile-up of 50) in 48 detector channels is a base for further considerations. Analog signals will be transmitted to the back-end electronics and then digitized by the 8 channel ADCs with a 1.25 GS/s sampling rate. Pairs of samples will be received at 625 MHz with DDR memory by a single FPGA.

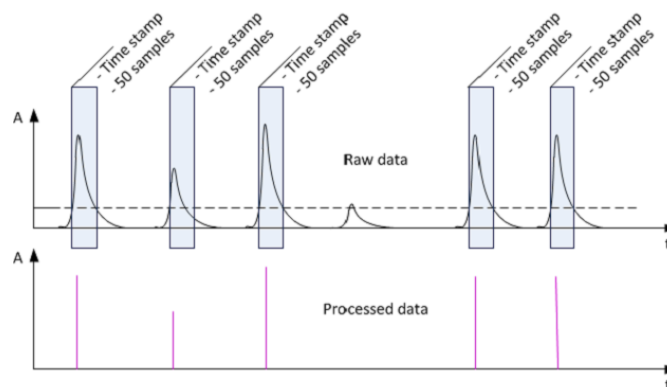


**Figure 4.** During one orbit of each Lumi Nibble raw data will be collected. After exceeding the threshold level, 50 consecutive 8-bit samples will be buffered.

## 2.1 Raw data

The statistical sample of the un processed data must be collected every LN for further offline processing. The minimum is 1 orbit/LN. Due to the limited FPGA resources it will be necessary to perform zero suppression. The data will be registered after exceeding the threshold level. 50 consecutive 8-bit samples will be buffered as is presented in figure 4. Each train of samples will be marked with a 17 bit time stamp coding its position in the orbit. The estimated data production for a single channel will be 390 kb, which gives the rate of 1.1 Mbit/s. For each processing board (4 channels) the data volume will be 1.6 Mbit and the rate 4.3 Mbit/s. In one crate 9.3 Mbit of the raw data will be stored and transmitted with the rate of 25.5 Mbit/s. For the BCM1F source data in BRIL DAQ the volume from 48 channels will be 18.6 Mbit incoming with about 50.9 Mbit/s.

## 2.2 Time domain histogram

The time domain histogram will provide information about the distribution of the hits in the LHC orbit. It will reflect the LHC bunch time structure observed on the basis of the incoming hits. A histogram will be filled during a LN interval and is aimed to provide the most reliable information about the collision particles and background. The possible resolution in time is from 4 to 8 bins/BX. Bins will be sent sequentially, including empty bins, which means that no time stamping will be required. For the 4 bins/BX resolution the data volume will be 6.9 kbit for 4 channels and 4.1 Mbit for one full crate. For the target 8 bins/BX the data volume is 1.4 Mbit for 4 channels and 8.3 Mbit for 24 channels.

## 2.3 The amplitude monitor of the gain

The energy loss of relativistic charged particles is described primarily by a Landau distribution. Activation products hit the sensors with low energies. If they are not well separated from the collision products, the distribution is shifted in the direction of the lower amplitudes. The amplitude histogram will be filled during the LHC orbit and integrated in LN, which will allow continuous monitoring of the performance of each channel. The calibration pulses for gain monitoring will be generated by the frontend ASIC calibration circuitry. The histogram will be filled with the amplitudes corresponding to the pre-defined test charge. The expected maximum number of counts

for the bin is  $2^{22}$ . The total data volume in 1 LN is 22.5 kbit for 4 channels and 135.2 kbit for 24 channels. The histogram may be divided into two separate parts, one for the normal counts and the second for the noise counts that can be continuously monitored. Bins will be sent sequentially, including empty bins.

**Table 1.** Data rates and volume in the different points of the system.

| <i>Data format</i>    | <i>GLIB processor</i>    | <i>AMC13 hub</i>           | <i>BRIL DAQ</i>            |
|-----------------------|--------------------------|----------------------------|----------------------------|
| Raw data              | 1.6 Mbit<br>(4.3 Mbit/s) | 9.3 Mbit<br>(25.5 Mbit/s)  | 18.6 Mbit<br>(50.9 Mbit/s) |
| Histogram (time)      | 1.4 Mbit                 | 8.3 Mbit                   | 16.6 Mbit                  |
| Histogram (amplitude) | 22.5 kbit                | 135.2 kbit                 | 270.3 kbit                 |
| Histograms in total   | 2.8 Mbit<br>(3.8 Mbit/s) | 16.8 Mbit<br>(22.8 Mbit/s) | 33.6 Mbit<br>(45.6 Mbit/s) |
| In total              | 4.3 Mbit<br>(8.1 Mbit/s) | 26.0 Mbit<br>(48.3 Mbit/s) | 52.0 Mbit<br>(96.5 Mbit/s) |

## 2.4 Total data production in Lumi Nibble

The total data production in a LN is presented in table 1. It is considered separately for the processing modules and the transmission modules. The data storage in the FPGA on the GLIB boards includes 4 detector channels, while the transmission to AMC13 includes 24 channels. The BRIL DAQ will receive data from all 48 channels. The total data storage of the raw data will be 1.6 Mbit in the GLIB and 18.6 Mbit in the DAQ. The data rate for each GLIB board will be 4.3 Mbit/s and for the AMC13 will be 25.5 Mbit/s. The time domain histogram will require the highest amount of block RAM in the FPGA. Storage of 4 channels requires 1.4 Mbit and all 48 channels 16.6 Mb. Storage of the amplitude histogram require only 22.5 kbit for 4 channels and 270.4 kbit for 48 channels. All histograms in the FPGA must be stored in a minimum of 2 buffers. The first buffer is used for the histogram that is currently being stored and second buffer for the previously collected histogram. The optional third buffer would provide an additional copy of the buffer in case of problems with transmission. In total the double buffers for histograms will take 2.8 Mbit in each GLIB board and 33.6 Mbit in the DAQ. The transmission rate will be 3.8 Mbit/s for the single GLIB and 22.8 Mbit/s for the AMC13. In total with the raw data from a single orbit the data size will be 4.3 Mbit for 4 channels transmitted with the 8.1 Mbit/s rate and 52.0 Mbit for 48 channels. The total transmission rate for one crate will be 48.3 Mbit/s. To provide the stable transmission of the data, the 10 Gbit/s transmission link of the AMC13 will be used. The trigger commands will be transmitted with the separate 80 Mbit/s link, so it was not taken into account for the estimation.

## 3 Identification of the hits

For this measurement the analogue signals will be converted by the ADCs on the custom modified FMC125 FMC board. The sampling clock will be synchronized to the LHC clock. The on-chip VCO will be configured into the frequency of 2484.96 MHz which gives a sampling rate



of 1242.48 MHz for each channel which corresponds to 31 samples for each bunch crossing. The trigger input of the board can be propagated to the FPGA and used for recognition of the first bunch crossing. The LHC orbit trigger will be provided.

### 3.1 Time and amplitude measurement methods

The pulse identification will be based on a time and amplitude measurement. A very high data rate and storage area required for the histograms will limit the possibility of implementing the complex mathematical methods in firmware. The strategy assumes an implementation of an online pulse identification methods based on peak finding and an offline statistical analysis of some amount of the raw data using a deconvolution method.

The impulse response of the front-end ASIC is given in Laplace domain by the following formula:

$$V_{\text{out}} \sim q_{\text{in}} \frac{1}{\left(1 + \frac{s}{\tau_{\text{pre}}}\right) \left(1 + \frac{s}{\text{GBW}_{\text{pre}}}\right) \left(1 + \frac{s}{\tau_{\text{sh}}}\right)}, \quad (3.1)$$

where  $\tau_{\text{pre}}$  is a time constant of the preamplifier,  $\text{GBW}_{\text{pre}}$  is a bandwidth that depends on the sensor capacitance and  $\tau_{\text{sh}}$  is a shaping time constant.

The preamplifier and the time constant affect the second order signal shaping. The  $\text{GBW}_{\text{pre}}$  is related to the transconductance of the input transistor and the sensor capacitance. This introduces a correction to the signal shape. The influence is non-negligible for higher values of the sensor capacitance. These parameters are being used for simulating the pulse identification algorithm with the following values:  $\tau_{\text{pre}} = 6$  ns,  $\tau_{\text{sh}} = 2.5$  ns and the inverse preamplifier bandwidth  $(\text{GBW}_{\text{pre}})^{-1} = 0.4$  ns at 2 pF capacitance respectively. The time domain response given by the inverse Laplace transform of formula (1) fits well to the measured pulse with a peaking time of 7 ns and FWHM of 9 ns.

The algorithm for online processing will be based on good knowledge of the signal characteristics as well as the transfer function of the system. The ASIC response for the signal corresponding to a Minimum Ionizing Particle (MIP) hit repeated with 12.5 ns spacing is presented in figure 5. The red signal has been measured directly on the output of the test board whereas the blue signal was measured on the output of the optical receiver. Both signals are distinguishable up to 10 ns in time spacing, so the result is better than expected.

The analysis of the signal after quantization and sampling was presented in [6]. The peak identification algorithm is able to distinguish pulses separated by 6 ns, so the time resolution will be limited by the hardware. The signal transmission path is currently being tested on the target hardware including the front-end PCBs that will be used in the experiment. Each transmission channel is being characterized separately. The ASIC characterization will provide important input values for the peak identification algorithm. One of the most important parameters will be the rise time of the signal. The peaking time of the pulses is the same independent of the energy of the particle hit and the amplitude of the generated pulse. This feature may be used for the identification of the missing peak in case of the overlap of the pulses of different amplitudes. The algorithm will be enhanced with noise filtering depending on the background characteristics and the baseline monitoring and measurement correction methods. This is currently being developed.

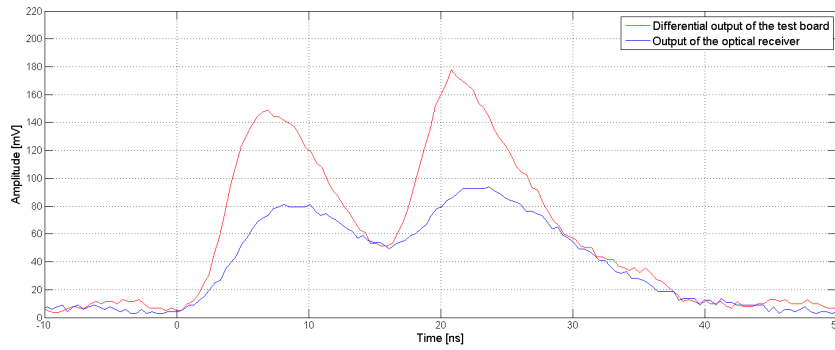


**Figure 5.** The output signal from the frontend ASIC corresponding to the Minimum Ionising Particle hit repeated after 12.5 ns measured on the output of the test board and on the output of the optical receiver.

### 3.2 Baseline monitoring

The baseline fluctuations can have an influence on the accuracy of the amplitude measurement. Baseline monitoring in the system will be performed in the last 500 ns of the abort gap within the orbit as presented in figure 6.  $A_{ref}$  (baseline) will be calculated. During collisions, a high hit rate may cause local dynamic baseline fluctuations because of the AC coupling of the ADCs. The local baseline level during collisions  $A_{ref}$  (dynamic) will be calculated. The difference of the reference levels values will be used as a correction factor to the absolute value of the measured amplitude  $A_{adc}$ .

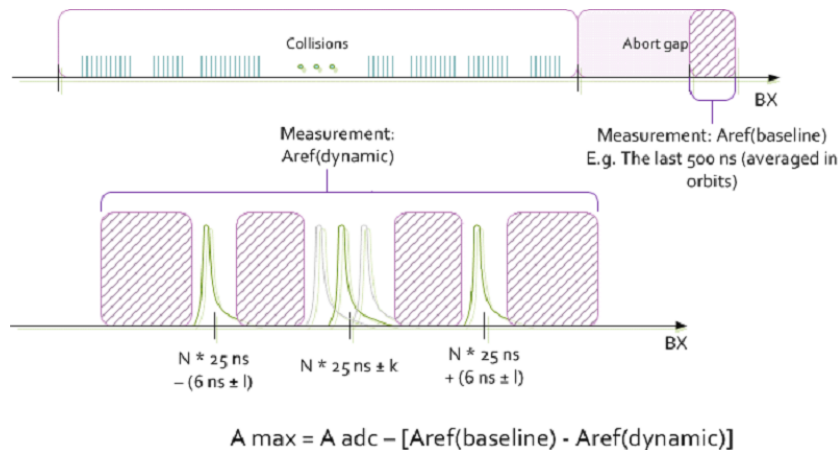


**Figure 6.** The last 500 ns of the abort gap  $A_{ref}$  (baseline) and dynamically (bottom) during collisions  $A_{ref}$  (dynamic). The measured peak amplitudes  $A_{adc}$  will be referenced to the baseline value.

**Summary.** The BCM1F system is upgraded for optimal performance after LS1. The frontend sensors consist of 24 single crystalline CVD diamond sensors with a two pad metallisation, positioned each end of the interaction point. The newly designed frontend ASIC comprising of a fast transimpedance preamplifier with an active feedback is able to generate pulses with less than 10 ns

FWHM. This will allow for an accurate separation of collision products from incoming machine induced background and activation products.

The architecture of the backend electronics system will be based on the MicroTCA technology and will allow for continuous processing of high data rates with a nanosecond resolution. The signals are received from the frontend electronics via 48 optical fibres. The AMC mother boards with custom FMC mezzanines will be used for the ADC conversion and signal processing. The LHC clock, LHC orbit trigger and the TCDS commands will be used for synchronisation and positioning of the measured peaks. The firmware design will be capable of processing signals at high input rates without introducing any dead time.

Occupancy and amplitude histograms and a pre-scaled selection of RAW data will be sent to the BRIL data acquisition system for processing of online luminosity and machine-induced-background algorithms.

## References

- [1] M. Hempel and B. Pollack, *Performance Analysis and Future Application of the Upgraded Fast Beam Condition Monitor at CMS*, at *International Beam Instrumentation Conference (IBIC) 2014*, Monterey U.S.A. (2014).
- [2] D. Przyborowski, *Design of a front-end ASIC for Single Crystal Diamond Sensors*, at *Applied Computational Electromagnetics Society (ACES) 2014 conference*, Jacksonville U.S.A. (2014).
- [3] Optical Links for CMS webpage, <http://cms-tk-opto.web.cern.ch/cms-tk-opto/>.
- [4] GLIB project public webpage, <https://espace.cern.ch/project-GLIB/public/default.aspx>.
- [5] A.J. Bell, *Beam & Radiation Monitoring for CMS*, *IEEE Nucl. Sci. Symp. Conf. Rec.* **2008** (2008) 2322.
- [6] A.A. Zagodzinska et al., *The Fast Beam Condition Monitor BCM1F Backend Electronics upgraded, MicroTCA based architecture*, *Proc. SPIE Int. Soc. Opt. Eng.* **9290** (2014) 92902L.
- [7] CACTUS project public webpage, <https://svnweb.cern.ch/trac/cactus>.
- [8] CMS collaboration, *The upgrade of the CMS trigger system*, *2014 JINST* **9** C08002.
- [9] G. Cervelli et al., *A radiation tolerant laser driver array for optical transmission in the LHC experiments*, in *Proceedings of the 7th LEB Workshop 2001*, Stockholm Sweden (2001), pg. 155.
- [10] V. Ryjov et al., *Fast Beam Conditions Monitoring (BCM1F) for CMS*, in *proceedings of Topical Workshop on Electronics for Particle Physics*, Naxos, Greece, 15–19 September 2008, pg. 259.
- [11] J.L. Leonard et al., *Upgraded Fast Beam Conditions Monitor for CMS online luminosity measurement*, *PoS(TIPP2014)* **346**, CMS CR-2014/108 (2014).
- [12] E. Bartz, *The 0.25  $\mu\text{m}$  token bit manager chip for the CMS pixel readout*, in *Proceedings of the 11th Workshop on Electronics for LHC and Future Experiments*, Heidelberg Germany (2005).